

Near-Infrared Fluorescent 9-Phenylethynylpyronin Analogues for Bioimaging

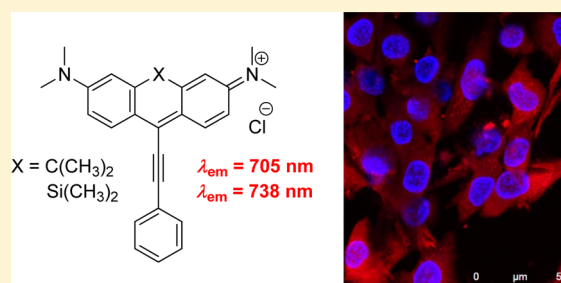
Tomáš Pastierik,^{†,‡} Peter Šebej,^{†,‡} Jiřina Medalová,[§] Peter Štacko,[†] and Petr Klán^{*,†,‡}

[†]Department of Chemistry and [‡]RECETOX, Faculty of Science, Masaryk University, Kamenice 5, 625 00 Brno, Czech Republic

[§]Department of Animal Physiology and Immunology, Institute of Experimental Biology, Faculty of Science, Masaryk University, Kotlarska 2, 611 37 Brno, Czech Republic

S Supporting Information

ABSTRACT: The syntheses and biological applications of two novel fluorescent 9-phenylethynylpyronin analogues containing either carbon or silicon at the position 10 are reported. Both fluorescent probes exhibited a relatively strong fluorescence in methanol and phosphate buffer saline in the near-infrared region (705–738 nm) upon irradiation of either of their absorption maxima in the blue and red regions. The compounds showed high selectivity toward mitochondria in myeloma cells in vivo and allowed their visualization in a favored tissue-transparent window, which makes them promising NIR fluorescent tags for applications in bioimaging.



INTRODUCTION

Organic fluorescent dyes are a ubiquitous part of molecular and biological sciences. They are frequently used as chemical sensors and biosensors and in bioimaging applications.^{1–4} Their popularity in biosciences has also attracted substantial attention from the synthetic community.^{5–8}

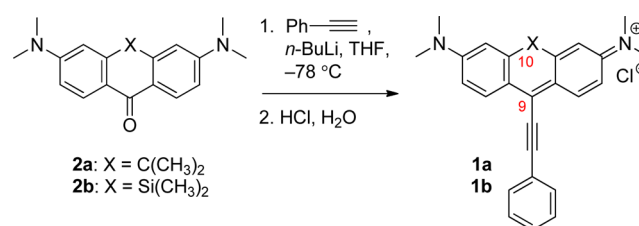
Rhodamines are highly favored fluorophores due to their advantageous photophysical properties, such as high molar absorption coefficients and fluorescence quantum yields and good aqueous photostability. Rhodamine 123 and tetramethylrhodamine ethyl ester (TMRE) are probably the most popular rhodamine derivatives used in flow cytometry and fluorescence microscopy at the present time. They are selectively sequestered in active mitochondria and thus often used as markers of the mitochondrial membrane potential (MMP).^{9–11} Monitoring the mitochondrial function is not the only application of these dyes as a decrease in the MMP is one of the earliest markers of apoptosis.¹² Rhodamine-based fluorophores are typically excited by a 488-nm argon laser and emit in the green or red regions, where they do not interfere with spectroscopic properties of other stains used to detect cellular parameters in bioimaging applications. Thus, far-red or near-infrared (NIR) emitting dyes with selective binding to various cell structures would open new possibilities in bioimaging.^{13,14} The first systems, such as Alexa Fluor 633, are already commercially available.

From a great variety of xanthenes and pyronin analogues currently known, only a few of them, such as the corresponding C9-alkyl,^{15–18} alkenyl,¹⁹ cyano,^{20,21} or carboxy²² derivatives, do not have aromatic substituents at the position C9. Recently, a patent describing preparation of 9-phenylethynylxanthenes and pyronin derivatives, structurally analogous to the C- and Si-

pyronin fluorophores presented in this work, has been claimed.²³

In this report, we describe the synthesis and photophysical properties of the novel 9-(phenylethynyl) C- and Si-pyronin NIR fluorophores **1a** and **1b** (Scheme 1). These molecules are

Scheme 1. Synthesis of 1a,b



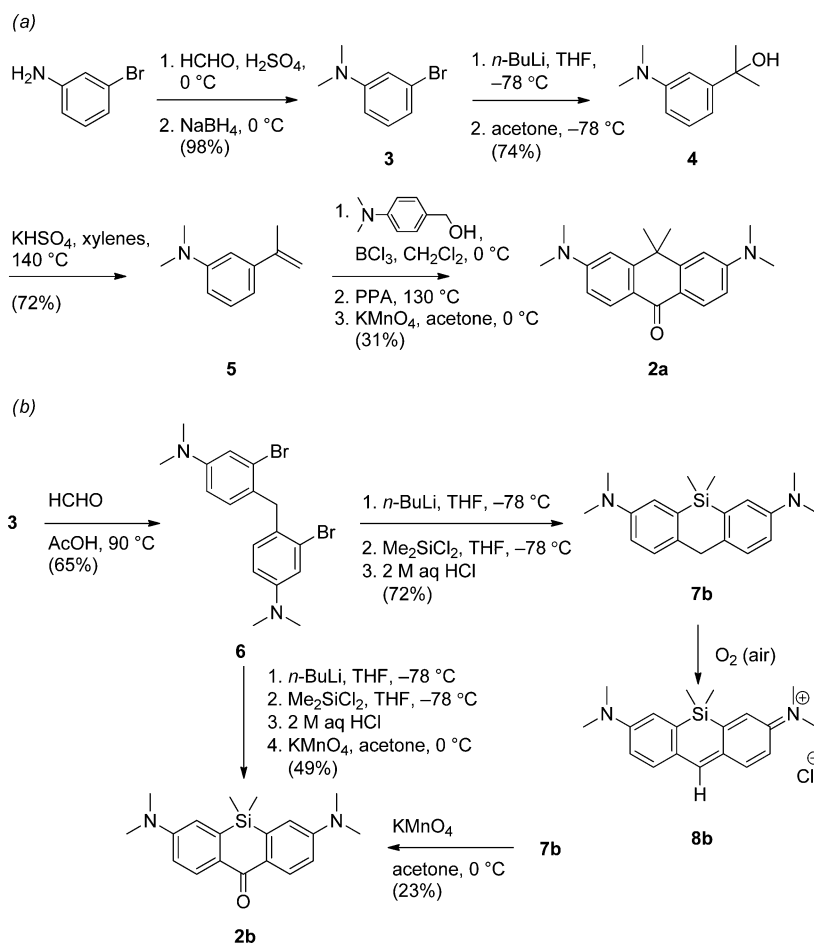
shown to permeate the cellular membrane allowing the visualization of mitochondria in vivo with the fluorescence bathochromically shifted to the near-infrared region in comparison to the common xanthenes- or rhodamine-based fluorophores.

RESULTS AND DISCUSSION

Synthesis. The two 9-phenylethynyl carbo- and silico-pyronin analogues **1a** and **1b** were synthesized by nucleophilic addition of a freshly prepared (phenylethynyl)lithium solution in THF at -78 °C to the carbonyl group of **2a** and **2b**, respectively, in good yields (61 and 83%, respectively; Scheme 1).

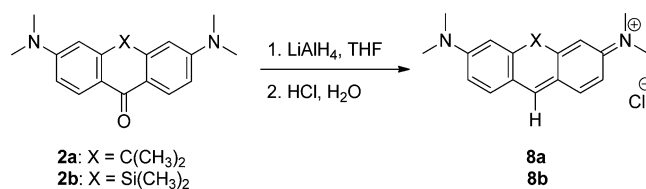
Received: January 20, 2014

Published: March 31, 2014

Scheme 2. Synthesis of (a) **2a** and (b) **2b**

The key intermediates **2a** and **2b** were prepared by different pathways. The starting 10,10-dimethylcaroxanthene-9-one (**2a**) was synthesized analogous to the procedure reported by Hell and co-workers²⁴ (Scheme 2a). Reductive amination of 3-bromoaniline, followed by nucleophilic addition of the resulting 3-bromo-*N,N*-dimethylaniline (**3**) to acetone, gave 2-(3-(dimethylamino)phenyl)propan-2-ol (**4**), which was dehydrated to form the synthetic precursor *N,N*-dimethyl-3-(prop-1-en-2-yl)aniline (**5**). Condensation of the two building blocks, **5** and (4-(dimethylamino)phenyl)methanol, in the presence of a Lewis acid (BCl_3 was found to be the most efficient) and subsequent cyclization of the adduct under dehydrating conditions followed by oxidation using KMnO_4 led to **2a** in 31% yield over the three steps. 10,10-Dimethylsilicoxanthene-9-one **2b** was synthesized by a procedure adopted from Nagano and co-workers (Scheme 2b).²⁵ The key synthetic intermediate, 4,4'-methylenebis(3-bromo-*N,N*-dimethylaniline) (**6**), was prepared by condensation of **3** with formaldehyde in 65% yield. The subsequent ring-closure reaction, a halogen–metal exchange reaction via a nucleophilic attack of 2,2'-methylenebis(arylolithium) to dichlorodimethylsilane, and oxidation of the reaction intermediate by KMnO_4 gave **2b** in 49% yield over the two steps. The reaction intermediate **7b** is isolable but relatively unstable; it is oxidized by air oxygen to give **8b** (Scheme 2b) which could not be further oxidized to **2b** by KMnO_4 . The direct synthesis of **2b** provided better yields (49%) compared to a stepwise method (**6** \rightarrow **7b** \rightarrow **2b**) in which the overall yield was 17%. The C- and Si-9H-pyrone

derivatives **8a, b** were also prepared by reduction of **2a, b** using LiAlH_4 (Scheme 3) as potential fluorescent impurities (see further in the text).

Scheme 3. Synthesis of **8a, b** from **2a, b**

Photophysical Properties. The 9-(phenylethynyl)pyrone analogues **1a, b** exhibited a strong absorption in the visible region (Figures 1 and 2, Table 1). The spectra of methanolic solutions possessed two characteristic absorption bands at $\lambda_{\text{abs}}^{\text{max}}$ (**1a**) = 472 and 677 nm and $\lambda_{\text{abs}}^{\text{max}}$ (**1b**) = 490 and 712 nm. The shape and relative intensities of the major absorption bands were not affected by the dye concentration (Figures S15 and S28, Supporting Information). The excitation spectra matched those of absorption (Figures 1 and 2). In contrast, the relative intensities of the two bands of **1** in phosphate buffer saline (PBS; pH = 7.4, $I = 0.1 \text{ mol dm}^{-3}$) in the region of 600–720 nm changed in the concentration range of 10^{-7} – $10^{-4} \text{ mol dm}^{-3}$ (Figures S14, S16, and S17 (**1a**) and S27, S29, and S30 (**1b**), Supporting Information). The spectra obtained at the lowest concentrations were dominated by the maxima at $\lambda_{\text{abs}}^{\text{max}}$

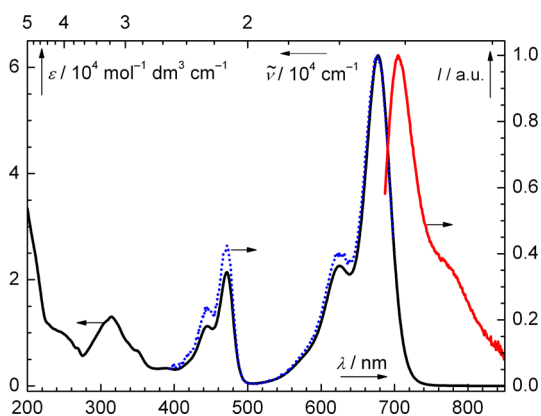


Figure 1. Absorption (black solid line), normalized emission ($\lambda_{\text{exc}} = 677$ nm; red solid line), and excitation ($\lambda_{\text{em}} = 708$ nm; blue dotted line) spectra of **1a** in methanol.

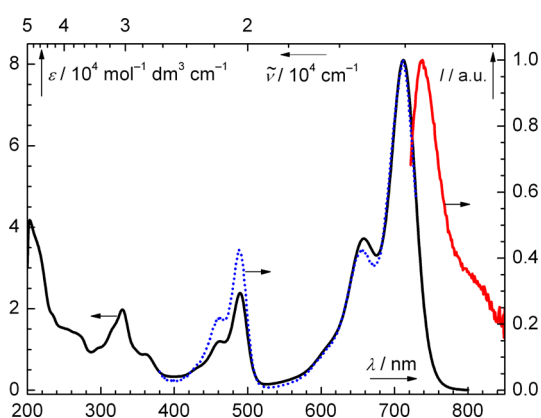


Figure 2. Absorption (black solid line), normalized emission ($\lambda_{\text{exc}} = 712$ nm; red solid line), and excitation ($\lambda_{\text{em}} = 738$ nm; blue dotted line) spectra of **1b** in methanol.

Table 1. Absorption and Emission Properties of **1a,b** in Methanol and PBS

dye	solvent	absorbance		fluorescence	
		$\lambda_{\text{abs}}^{\text{max}}/\text{nm}$	$\log \epsilon^{\text{a}}$	$\lambda_{\text{em}}^{\text{max}}/\text{nm}$	$\Phi_{\text{f}}(\lambda_{\text{exc}}/\text{nm})^{\text{b}}$
1a	MeOH	472	4.33	705	0.135 ± 0.013 (472)
		677	4.79	705	0.148 ± 0.014 (625)
	PBS ^{c,d}	476	4.22	710	0.016 ± 0.007 (484) ^e
		680	4.60	708	0.017 ± 0.002 (633) ^e
1b	MeOH	490	4.38	738	0.066 ± 0.011 (490)
		712	4.91	738	0.070 ± 0.008 (657)
	PBS ^{c,d}	492	4.45	735	0.004 ± 0.002 (493) ^f
		712	4.75	736	0.004 ± 0.002 (670) ^f

^a $\log [\epsilon/\text{mol dm}^{-3} \text{cm}^{-1}]$. ^bThe fluorescence quantum yield (Φ_{f}) values are the averages of five measurements. The standard deviations and the excitation wavelengths (λ_{exc}) are shown. ^cDMSO (1%, v/v) was used as a cosolvent due to low solubilities of **1a,b** in water. ^dThe absorption characteristics were measured at $c < 5 \times 10^{-6}$ mol dm⁻³ to ensure that the monomeric form prevails. ^eA PBS/DMSO (39:1, v/v) mixture was used as a solvent. ^fA PBS/DMSO (999:1, v/v) mixture was used as a solvent.

(**1a**) = 680 nm and $\lambda_{\text{abs}}^{\text{max}}$ (**1b**) = 712 nm. However, the new maxima at 607 and 652 nm for **1a** and **1b**, respectively, appeared at higher dye concentrations ($c > 5 \times 10^{-6}$ mol dm⁻³). This behavior is usually associated with dye aggregation in polar media^{26–28} and their lower solubilities in aqueous

solutions. Such hypsochromically shifted bands suggest that H-aggregates are formed, which have also been observed in the case of other pyronin derivatives.^{27,29}

The NIR emission bands at $\lambda_{\text{em}}^{\text{max}} = 705$ and 738 nm in methanol (and 708 and 736 nm in PBS) for **1a** and **1b**, respectively, were obtained upon excitation to both absorption maxima (Table 1; Figures 1 and 2; Figures S13 and S26, Supporting Information). The position and shape of the emission maxima were not affected by the dye concentration in either solvent. The fluorescence quantum yields were found to be reasonably high in methanol ($\Phi = 0.07$ – 0.15) and approximately 1 order of magnitude lower in PBS (Table 1). Their values were essentially independent of the excitation wavelength and are comparable to those of commercially available rhodamine dyes, such as ATTO 725 ($\Phi = 0.10$)³⁰ or Alexa Fluor 750 ($\Phi = 0.10$),³¹ which fluoresce in the NIR region. The fluorescence decay of **1b** in a methanolic solution obeyed a single exponential rate law ($\tau_{1\text{b}} = 1.0 \pm 0.3$ ns).

Both absorption and emission maxima of **1a,b** are shifted bathochromically compared to the analogues possessing oxygen at the position 10 as has been reported for a 9-(mesitylethynyl)pyronin derivative²³ or other pyronin analogues.^{25,32,33} The difference in $\lambda_{\text{em}}^{\text{max}}$ between **1a** and **1b** is analogous to that observed for fluorescein and rhodamine derivatives, possibly reflecting a different stabilization of the LUMO energies of the two fluorophores.^{25,32}

The optical properties of **1a,b** were also determined in a suspension of living HL-60 cells in the RPMI-1640 media in connection with our bioimaging studies described further in the text. The effect of the cell microenvironment was found to be negligible: both the emission and excitation spectra were nearly identical to those obtained in PBS. The fluorescence quantum yields ($\sim 1\%$) were also similar; however, this value can only be estimated due to the complexity and heterogeneity of the system.

Stability. The chemical stability of **1a,b** in the dark was found to be reasonable in all solvents used (PBS, DMSO, water, or methanol; see also the Supporting Information). For example, only ~ 2 and 4% of **1a** and **1b**, respectively, decomposed in a PBS solution ($c \sim 10^{-5}$ mol dm⁻³) in 12 h at 20 °C; degradation of the dyes in aq methanol was faster by a factor of ~ 8 . High-resolution mass spectrometric analyses of a solution of **1b** in methanol kept in the dark for several days indicated that **8b** and **2b** are the degradation products (Figure S38, Supporting Information). The stability of **1a,b** in frozen DMSO solutions and in a sample containing HL-60 cells in the RPMI-1640 media was also tested (see further in the text and the Supporting Information).

Both **1a** and **1b** in methanol ($c \sim 10^{-5}$ mol dm⁻³) decomposed completely upon irradiation with 32 high-energy LEDs ($\lambda_{\text{em}} = 653$ nm; see the Experimental Section) within 60 min. The major photoproduct was determined to be 9-methoxyppyronin in both cases based on an HR-MS analysis (Figure S39, Supporting Information), which was also formed upon irradiation of 9-(1,3-dithian-2-yl)pyronins.¹⁶

Fluorescent Impurities. After cautious purification by chromatography on silica and reversed-phase silica, both compounds **1a,b** still contained a small amount ($< 1\%$) of the corresponding 9H-pyronins **8a,b** detectable only by the fluorescence spectroscopy in PBS solutions but undetectable by both UV-vis and NMR. Their identification was based on their comparison with the authentic compounds synthesized independently from **2a,b** (Scheme 3). Compounds **8a,b**

exhibited a strong absorption in the visible region; however, in contrast to **1a,b**, they possessed only one absorption band at $\lambda_{\text{abs}}^{\text{max}} = 605$ and 636 nm, respectively, in methanol. The far-red emission bands with $\lambda_{\text{em}}^{\text{max}} = 620$ and 648 nm, respectively, found in methanol solutions were recorded upon excitation at their absorption maxima (Figure S33 and S36, Supporting Information).

Bioimaging. In bioimaging applications, there is a need for light-emitting probes which possess large molar absorption coefficients, high quantum yields of emission, preferably in the tissue-transparent window (700–1000 nm),³⁴ and large Stokes shifts. They should be sufficiently photostable and resistant to degradation in biological systems. A large Stokes shift can prevent self-quenching and measurement errors caused by excitation and scattered light³⁵ and facilitate multichannel bioimaging.³⁶ Large Stokes shifts (>100 nm) are common for inorganic phosphorescent heavy-metal complexes³⁷ but relatively rare for small organic monochromophoric fluorescent probes, such as BODIPY,^{38,39} cyanines,⁴⁰ or UV-absorbing 2,3-naphthalimide⁴¹ derivatives. We found that the relatively small (but typical for rhodamine fluorophores) Stokes shifts of ~ 27 nm observed upon irradiation of **1a,b** at the major absorption bands can be overcome by excitation at the second absorption band at $\lambda_{\text{abs}}^{\text{max}} \sim 480$ nm, related probably to the extended π -conjugation of the pyronin chromophore with the 9-phenylethynyl group, providing the same emission in the NIR region. In such a case, the gap between the absorption and emission maxima is very large (233 and 247 nm for **1a,b**, respectively), comparable to that of large pseudo-Stokes shifts reported for bichromophoric tandem dyes^{42,43} and fluorescent proteins.⁴⁴ This also allows utilization of a common 488 nm argon laser as a source of the excitation light with concomitant detection in the near-infrared region. Although the molar absorption coefficients at the band maxima at ~ 480 nm ($\epsilon \sim 25000$ mol⁻¹ dm³ cm⁻¹) are lower compared to those of the major bands by a factor of 3, we have not registered any detrimental reduction of the fluorescence signal levels in our bioimaging experiments described in the subsequent paragraph. In addition, dual band excitation properties of **1a,b** offer an opportunity to selectively identify these fluorescence probes in a more complex system and in the presence of different fluorophores.

In order to test our novel fluorescent probes for bioimaging, staining of live cells was studied using confocal fluorescent microscopy. The excitation of **1a,b** by either of the 488 and 670 nm laser beams led to a strong emission in the NIR region (Figure 3; individual fluorescence images of **1a, b** and DAPI are provided in Figures S41 and S42, Supporting Information). These excitation wavelengths were chosen to emphasize the most important spectroscopic feature of both **1a** and **b**, an identical fluorescence observed upon excitation either of the major absorption bands in the visible region. Furthermore, using a NIR emission channel suppressed unwanted cellular autofluorescence. These absorption wavelengths allowed us to avoid accidental excitation of the trace impurities **8a,b** (see above).

Staining of cells with both dyes was rapid; the maximal fluorescence intensity, determined by time-lapse flow cytometry analyses, was reached in less than 2 min of incubation at 20 °C at an optimized dye concentration (~ 0.01 mg mL⁻¹; Figures S43 and S44, Supporting Information). The fluorescence intensity of **1a,b** in the cell samples was stable during all flow cytometric (Figures S43b, S43d, S44b, and S44d, Supporting

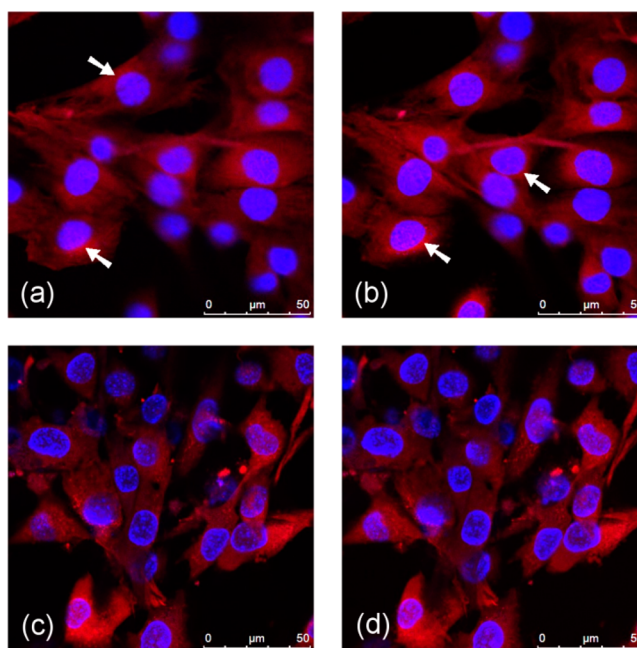


Figure 3. Overlay images of mouse skeletal myoblast C2C12 stained with 4',6-diamidino-2-phenylindole (DAPI; $\lambda_{\text{exc}} = 405$ nm, $\lambda_{\text{em}} = 460$ nm), localized in the cell nuclei (blue fluorescence) and **1** (a: **1a**, $\lambda_{\text{exc}} = 488$ nm; b: **1a**, $\lambda_{\text{exc}} = 670$ nm; c: **1b**, $\lambda_{\text{exc}} = 488$ nm; d: **1b**, $\lambda_{\text{exc}} = 670$ nm). All images were obtained by confocal fluorescence microscopy using the same emission filter of 700–800 nm (red fluorescence); the arrows highlight the perinuclear staining; the scale bar is 50 μm .

Information) and fluorescent microscopy analyses, which implies that their concentrations did not decline markedly during the experiments. In addition, we aimed to assess the intracellular localization of the probes by confocal microscopy that captures cross-sections of observed cells. Compound **1b** stained almost uniformly the whole cytoplasm and nucleus. On the other hand, **1a** had a staining pattern similar to that of the JC-1 mitochondrial stain (Figure S40, Supporting Information); that is, the dye was concentrated mainly in the perinuclear space where mitochondria are located. Small foci created by stained mitochondrial clusters were also observed (Figure 3). The cytotoxicity of **1a,b** was evaluated by the flow cytometry analysis. The extent of apoptotic cell death, characterized by changes in cell shape and size, was determined as a decrease in the FSC (forward-light scatter) signal values (Figure S45, Supporting Information). Our analysis showed that both dyes were only slightly cytotoxic.

CONCLUSIONS

Two novel 9-phenylethynyl C- and Si-pyronin analogues **1a,b** were synthesized and their emission properties studied. Both compounds exhibited a relative strong fluorescence in the NIR region when irradiated at either of the two major absorption bands in the visible region. In addition, the compounds showed high selectivity toward mitochondria in myeloma cells in vivo and allowed their visualization in a tissue-transparent window. Characteristic and favorable photophysical properties of **1a,b** can thus give the researcher freedom to choose the excitation wavelength available for a bioimaging experiment and make them suitable for multichannel fluorescence microscopy and multicolor fluorescence applications. Further applications of 9-phenylethynyl-pyronin dyes are currently under investigation in our laboratories.

EXPERIMENTAL SECTION

Materials and Methods. Reagents and solvents of the highest purity available were used as purchased. Acetone and dichloromethane were dried by standard procedures, kept over activated 3 Å molecular sieve (8–12 mesh) under dry N₂, and freshly distilled before each experiment. Tetrahydrofuran was dried with sodium, stored over sodium benzophenone ketyl, and freshly distilled before each experiment. Phosphate buffer saline was prepared by a 1:10 dilution of the stock solution of PBS (prepared by direct weighting of NaCl (80 g), KCl (2.0 g), Na₂HPO₄·12H₂O (23 g), and KH₂PO₄ (2.4 g) into a volumetric flask which was filled with distilled water to 1 L).

The synthetic steps were performed under ambient atmosphere unless stated otherwise. All glassware was oven-dried prior to use when water- and/or air-sensitive reagents were used. The Schlenk techniques were utilized when working with air and/or moisture sensitive chemicals. All column chromatography purification procedures were performed on columns packed with silica gel 60 (40–63 μm).

The NMR spectra (Supporting Information) were recorded on 300 and 500 MHz spectrometers in chloroform-*d*, dimethylsulfoxide-*d*₆, methanol-*d*₄, and water-*d*₂. The signals in ¹H and ¹³C NMR spectra were referenced⁴⁵ to the residual peak of a deuterated solvent. The deuterated solvents except water-*d*₂ were kept over activated 3 Å molecular sieve (8–12 mesh) under dry N₂. The mass spectra were recorded on a GC-coupled (a 30 m DB-XLB column) spectrometer in a positive mode with EI (70 eV) or FAB. A mass spectrometer equipped with a N₂ laser (λ = 337 nm) with output set to ~3 mW was used for MALDI analyses; a mass detector was calibrated with red phosphorus. The UV–vis spectra were obtained with matched 0.1, 1.0, and 5.0 cm quartz cells. IR spectra were obtained on a FT spectrometer using ATR or KBr pellets. The exact masses were obtained using a triple quadrupole electrospray ionization mass spectrometer in positive or negative modes. Melting points were obtained using a noncalibrated Kofler's hot stage melting point apparatus. The solution pH values were determined using a glass electrode calibrated with certified buffer solutions at pH = 4, 7, or 10. Fluorescence was measured on an automated luminescence spectrometer in 1.0 cm quartz fluorescence cuvettes at 26 ± 1 °C; the sample concentration was set to keep the absorbance below 0.1 at λ_{max}; each sample was measured five times, and the corrected spectra were averaged. In some cases (cell suspensions), the dye concentration was set to 0.01 mg mL⁻¹ (A(λ_{max}) ~ 0.5) and the fluorescence was measured in a front-face mode to eliminate reabsorption of the emitted light. A front-face mode was also employed to determine the concentration dependence of the emission spectra. Emission and excitation spectra are normalized; they were corrected using standard correction files. Fluorescence quantum yields were determined as the absolute values in 1.0 cm quartz fluorescence cuvettes at 26 ± 1 °C using an integration sphere. For each sample, the quantum yield was measured five times, and the values were averaged. A nanosecond flash lamp (filled with H₂) was used for measurements of the fluorescence lifetimes. The data obtained were deconvoluted from the corresponding measured decay curves and an instrumental response function.

Thermal Stability. The chemical stability of **1a,b** (c ~ 1 × 10⁻⁵ mol dm⁻³, A = 1.0 ± 0.2 at λ_{abs}^{max}) in methanol, DMSO, water, and PBS (pH = 7.4, I = 0.1 mol dm⁻³) solutions in the dark at 20 °C was tested using UV–vis spectroscopy.

Irradiation Experiments. A solution of **1** (c ~ 10⁻⁵ mol dm⁻³, A (at λ_{abs}^{max}) = 1.0) in nondried methanol (3 mL) in a matched 1.0 cm quartz cuvette was irradiated at 20 °C using a homemade light source equipped with 32 high-energy LEDs emitting at λ_{em} = 653 ± 11 nm (power dissipation of 1 LED: 100 mW; the bandwidth at half-height = 22 nm; its spectrum is shown in Figure S39b, Supporting Information) until **1** disappeared. The reaction progress was monitored by UV–vis spectrometry using a diode-array spectrometer, and the final reaction mixture was further analyzed by HRMS.

Bioimaging Experiments. The leukemic cell line HL-60 (ATCC) cultivated in RPMI1640 media supplemented with 10% fetal bovine serum, streptomycin (0.1 mg mL⁻¹), penicillin (100 U mL⁻¹), and L-

glutamine (3.3 mmol L⁻¹) was used for the flow cytometry analyses. A suspension of cells was stained by **1a,b** and **8a,b** in concentrations of 0–1 mg mL⁻¹. The medians of fluorescence intensities in all the spectral regions (λ_{exc} = 488 nm: λ_{obs}(fl) = 530 ± 30 nm (FL-1), λ_{obs}(fl) = 585 ± 40 nm (FL-2) and λ_{obs}(fl) = 670 nm long pass (FL-3); λ_{exc} = 630 nm: λ_{obs}(fl) = 675 ± 25 nm (FL-4)) together with the time lapse measurements (0–3 min) were evaluated on a flow cytometer.

A flow cytometry assessment of live HL-60 cells stained with each individual compound **1a,b** and **8a,b** (c = 0.01 mg mL⁻¹) showed that fluorescence of **8** in vivo has a 5-fold to hundred-fold lower intensity than that of the analogous pyronin **1** (Figures S43 and S44, Supporting Information), which ensured that no fluorescence interference from **8a,b** (<1% dye content) occurred in the study samples.

The microscopic evaluation and cytotoxicity assessment were performed on mouse skeletal myoblast C2C12 (ATCC) grown on coverslips in DMEM media, supplemented with 10% fetal bovine serum, streptomycin (0.1 mg mL⁻¹), penicillin (100 U mL⁻¹), and L-glutamine (3.3 mM). The cell staining by **1a,b** (0.02 mg mL⁻¹) was performed for 3 min at 20 °C, and then the coverslips were mounted in glycerol and the specimens observed by a confocal microscope. Nuclei were prestained by DAPI (the final concentration was 5 μg mL⁻¹) and mitochondria by JC-1 (0.125 μg mL⁻¹) for 20 min at 37 °C.

Synthesis of 3,6-Bis(dimethylamino)-10,10-dimethylanthracen-9(10H)-one (2a). 3-Bromo-*N,N*-dimethylaniline (**3**). Aqueous H₂SO₄ (3 M, 56 mL) was added to a stirred solution of aq formaldehyde (37%, 20.8 mL, 279 mmol) in tetrahydrofuran (250 mL), and the mixture was cooled to 0 °C and stirred for another 10 min. 3-Bromoaniline (16 g, 93 mmol) was then added dropwise within 10 min, and the reaction mixture was stirred for an additional 10 min. Solid NaBH₄ (14.1 g, 372 mmol) was slowly added portionwise within 30 min while the temperature was maintained at 0 °C. The resulting mixture was allowed to warm and stirred for 1 h at 20 °C. Saturated aq NaHCO₃ (350 mL) was then added, and the reaction mixture was extracted with CH₂Cl₂ (3 × 100 mL). The combined organic layers were dried over anhydrous MgSO₄ and filtered, and solvents were evaporated under reduced pressure. The crude product was of sufficient purity for the next step. Yield: 18.5 g (98%). Yellowish liquid. ¹H NMR (300 MHz, CDCl₃): δ (ppm) 2.98 (s, 6H), 6.68 (dd, 1H, J₁ = 8.7 Hz, J₂ = 1.9 Hz), 6.88–6.90 (m, 2H), 7.14 (t, 1H, J = 8.0 Hz) (Figure S1, Supporting Information). ¹³C NMR (75.5 MHz, CDCl₃): δ (ppm) 40.5, 111.1, 115.3, 119.3, 123.6, 130.4, 151.9 (Figure S2, Supporting Information). FTIR (KBr, cm⁻¹): 2985, 2937, 2885, 2804, 1595, 1554, 1498, 1443, 1354, 1230, 1180, 1095, 1066, 983, 957, 829, 783, 758, 681, 660, 440. MS (EI): 202 (7), 201 (90), 200 (100), 199 (95), 198 (98), 185 (10), 155 (10), 118 (30), 104 (20), 91 (10), 77 (20), 63 (10), 50 (1), 42 (12) 27(3). This compound has also been characterized elsewhere.⁴⁶

2-(3-(Dimethylamino)phenyl)propan-2-ol (**4**). *n*-Butyllithium (2.5 M solution in cyclohexane, 4.00 mL, 10.0 mmol) was added dropwise to a solution of 3-bromo-*N,N*-dimethylaniline (**3**, 2.00 g, 10.0 mmol) in dry tetrahydrofuran (40 mL) in a Schlenk tube during 15 min at -78 °C under dry N₂ atmosphere. The reaction mixture was stirred for 15 min, and dry acetone (0.734 mL, 10.0 mmol) was added in two portions at -78 °C. The stirring continued for another 15 min at this temperature, and the temperature was subsequently allowed to rise to 20 °C. The reaction was quenched by dropwise addition of aq HCl (10 mL, 2 M), and the solution was neutralized to pH 7 with satd aq NaHCO₃ (~ 25 mL). The reaction mixture was then extracted with dichloromethane (3 × 50 mL). The combined organic layers were dried over anhydrous MgSO₄ and filtered, and the solvents were removed under reduced pressure. Column chromatography (ethyl acetate/*n*-hexane, 1:5, v/v) gave the pure product. Yield: 1.32 g (74%). Colorless crystals. Mp: 72–74 °C (lit.⁴⁷ mp 72–73 °C). ¹H NMR (300 MHz, CDCl₃): δ (ppm) 1.61 (s, 6H), 1.89 (s, 1H, -OH), 2.99 (s, 6H), 6.66 (ddd, 1H, J₁ = 8.3 Hz, J₂ = 2.6 Hz, J₃ = 0.6 Hz), 6.83 (ddd, 1H, J₁ = 7.7 Hz, J₂ = 1.6 Hz, J₃ = 0.8 Hz), 6.96–6.97 (m, 1H), 7.24 (t, 1H, J = 8.0 Hz) (Figure S3, Supporting Information). ¹³C NMR (75.5 MHz, CDCl₃): δ (ppm) 31.9, 40.9, 72.9, 109.0, 111.3, 113.1, 129.1, 150.4, 150.9 (Figure S4, Supporting Information). FTIR

(KBr, cm^{-1}): 3344 (br), 2974, 2935, 2872, 2845, 2804, 1603, 1576, 1493, 1433, 1402, 1375, 1348, 1230, 1182, 1138, 1088, 1061, 995, 955, 881, 862, 793, 775, 702, 679, 565, 484. MS (EI): 179 (83), 178 (12), 164 (16), 162 (13), 148 (3), 134 (4), 122 (100), 120 (28), 107 (18), 91 (8), 81 (4), 77 (12), 63 (7), 43 (22). This compound has also been characterized elsewhere.⁴⁸

***N,N*-Dimethyl-3-(prop-1-en-2-yl)aniline (5)**. A suspension of 2-(3-(dimethylamino)phenyl)propan-2-ol (4, 1.24 g, 6.92 mmol) and potassium hydrogen sulfate (0.942 g, 6.92 mmol) in xylenes (7 mL) was stirred in a pressure tube at 150 °C for 1 h. The reaction mixture was cooled to 20 °C, water (20 mL) was added, and the mixture was stirred until an inorganic precipitate was dissolved. The pH of the reaction mixture was adjusted to ~8 by dropwise addition of aq NaOH (20%, w/w), and the organic material was extracted with dichloromethane (3 × 50 mL). The combined organic layers were dried over anhydrous MgSO_4 and filtered, and the solvents were removed under reduced pressure to give a brown oil. Column chromatography (ethyl acetate/*n*-hexane, 1:50, stepwise changed to 1:5, v/v) gave the pure product. Yield: 803 mg (72%). Colorless oil. ¹H NMR (300 MHz, CDCl_3): δ (ppm) 2.18 (s, 3H), 2.99 (s, 6H), 5.08 (s, 1H), 5.36 (s, 1H), 6.68–6.74 (m, 1H), 6.84–6.89 (m, 2H), 7.23 (t, 1H, $J = 8.2$ Hz) (Figure S5, Supporting Information). ¹³C NMR (75.5 MHz, CDCl_3): δ (ppm) 22.3, 41.0, 110.4, 112.3, 112.3, 114.7, 129.1, 142.6, 144.6, 150.9 (Figure S6, Supporting Information). FTIR (KBr, cm^{-1}) = 3084, 2970, 2945, 2914, 2885, 2843, 2800, 1599, 1574, 1498, 1433, 1350, 1230, 1182, 1120, 1061, 995, 970, 889, 849, 779, 725, 685, 548, 523, 442. MS (EI): 162 (8), 161 (82), 160 (100), 144 (7), 130 (5), 118 (6), 115 (13), 102 (4), 91 (9), 77 (7), 63 (4), 51 (3), 42 (3). This compound has also been characterized elsewhere.^{49,50}

4-(Dimethylamino)phenyl)methanol. Lithium aluminum hydride (22.9 g, 0.60 mol) in dry tetrahydrofuran (500 mL) was added dropwise to a solution of 4-(dimethylamino)benzaldehyde (45 g, 0.30 mol) in dry tetrahydrofuran (60 mL) at 0 °C. The mixture was stirred for 3 h, and then water (23 mL), aq NaOH (23 mL, 15%, w/w), and water (70 mL) were added slowly in sequence (caution: hydrogen is evolving during this procedure). The mixture was stirred for another 30 min at 0 °C and filtered through a thin pad of silica. The filtrate was extracted with dichloromethane (3 × 50 mL). Mixed organic layers were dried over anhydrous MgSO_4 and filtered, and the solvents were removed under reduced pressure to give the title product. No further purification was necessary. Yield: 43.5 g (95%). Yellowish viscous oil, slowly crystallizing in a freezer. Mp <25 °C (lit.⁵¹ mp 22–24 °C). ¹H NMR (300 MHz, CDCl_3): δ (ppm) 2.90 (s, 1H, -OH), 2.97 (s, 6H), 4.55 (s, 2H), 6.77 (d, 2H, $J = 8.8$ Hz), 7.26 (d, 2H, $J = 8.8$ Hz) (Figure S7, Supporting Information). ¹³C NMR (75.5 MHz, CDCl_3): δ (ppm) 40.7, 64.9, 112.8, 128.5, 129.3, 150.2 (Figure S8, Supporting Information). FTIR (neat on a Teflon foil, cm^{-1}): 3379, 2862, 2800, 1612, 1568, 1522, 1477, 1444, 1344, 1230, 1186, 1163, 1130, 1016, 944, 804, 739, 692, 563, 511. MS (EI): 151 (80), 134 (100), 120 (10), 107 (10), 91 (4), 77 (7). This compound has also been characterized elsewhere.^{52,53}

3,6-Bis(dimethylamino)-10,10-dimethylanthracen-9(10H)-one (2a). Boron trichloride (1 M solution in dichloromethane, 23.5 mL, 23.5 mmol) was added dropwise to a solution of 4-(dimethylamino)phenyl)methanol (3.09 g, 20.5 mmol) and *N,N*-dimethyl-3-(prop-1-en-2-yl)aniline (5, 3.30 g, 20.5 mmol) in dry dichloromethane (100 mL) at 0 °C under dry N_2 atmosphere over 15 min. The reaction mixture was stirred overnight and was allowed to warm to 20 °C. Polyphosphoric acid ($\geq 83\%$ phosphate (as P_2O_5), 50 g) was then added to the reaction mixture. The mixture was warmed to 40 °C, and dichloromethane was allowed to slowly evaporate through a thick cannula under slow flow of N_2 . The reaction mixture was then heated to 130 °C, and the viscous material was stirred for an additional 3 h. The reaction mixture was allowed to cool to 20 °C, poured onto ice (0.5 kg) in a beaker, neutralized with cold aq NaOH (20%, w/w), and extracted with dichloromethane (4 × 100 mL). The combined organic layers were concentrated under reduced pressure to ~100 mL and washed with aq $\text{Na}_2\text{S}_2\text{O}_3$ (25 mL, 10%). The organic layer was then separated, and the solvent was removed under reduced pressure to give a yellow viscous residue (6.80 g).

Powdered potassium permanganate (6.80 g, 43.0 mmol) was added portionwise to a solution of the above-described crude product (20.5 mmol) in acetone (150 mL) at 0 °C over 2 h. The reaction mixture was stirred for another 1 h (the reaction progress was monitored by TLC). When no starting material was observed, the reaction mixture was filtered through a short pad of silica gel to remove MnO_2 , and the pad was thoroughly washed with chloroform (1.4 L). The filtrate was collected, and the solvents were evaporated to give a green crystalline powder. Column chromatography (*n*-hexane/ethyl acetate/chloroform, 5:1:1, v/v) gave the pure product. Yield: 1.90 g (31%). Yellowish crystalline solid. Mp: 233–234.5 °C. ¹H NMR (300 MHz, CDCl_3): δ (ppm) 1.73 (s, 6H), 3.10 (s, 12H), 6.73–6.80 (m, 4H), 8.28 (dd, 2H, $J_1 = 8.3$ Hz, $J_2 = 0.6$ Hz) (Figure S9, Supporting Information). ¹³C NMR (75.5 MHz, CDCl_3): δ (ppm) 33.9, 38.4, 40.3, 108.0, 111.0, 120.2, 129.3, 152.5, 153.3, 181.3 (Figure S10, Supporting Information). FTIR (KBr, cm^{-1}): 3078, 2981, 2968, 2935, 2910, 2808, 1595, 1520, 1444, 1433, 1367, 1333, 1217, 1078, 966, 929, 850, 831, 781, 694, 582, 509. MS (EI): 308 (95), 293 (100), 277 (14), 265 (13), 250 (9), 221 (13), 178 (12), 140 (22), 132 (26), 95 (16), 81 (24), 69 (45), 41 (30). HRMS (APCI⁺): calcd for $\text{C}_{20}\text{H}_{25}\text{N}_2\text{O}$ ($M + \text{H}^+$) 309.1961, found 309.1967.

***N*-(7-(Dimethylamino)-9,9-dimethyl-10-(phenylethynyl)anthracen-2(9H)-ylidene)-*N*-methylmethanaminium Chloride (1a)**. *n*-Butyllithium (2.2 M solution in cyclohexane, 1.4 mL, 3.08 mmol) was added dropwise to a solution of phenylacetylene (0.37 mL, 3.39 mmol) in dry tetrahydrofuran (10 mL) in a Schlenk tube under dry N_2 atmosphere at -78 °C. The reaction mixture was stirred for 30 min, and a solution of 3,6-bis(dimethylamino)-10,10-dimethylanthracen-9(10H)-one (2a, 190 mg, 0.616 mmol) in dry tetrahydrofuran (10 mL) was subsequently added dropwise. The reaction mixture was stirred at -78 °C for 1 h and then stirred overnight while the temperature was allowed to rise to 20 °C. The reaction was quenched by satd aq NH_4Cl (3 mL), and aq HCl (2 M, 0.7 mL) was subsequently added dropwise to the reaction mixture. After being stirred for 5 min, the mixture was extracted with dichloromethane (10 mL). Green solid precipitated in a separatory funnel. The organic layer was carefully separated and discarded. An aqueous layer and the solid were then washed with dichloromethane (3 × 10 mL) to dissolve the precipitate. The organic layers were combined and dried over anhydrous MgSO_4 . The solvents were removed under reduced pressure to give the pure title product. Yield 160 mg (61%). Dark green solid. Mp: 231–233 °C. ¹H NMR (300 MHz, CDCl_3): δ (ppm) 1.81 (s, 6H), 3.48 (s, 12H), 6.98 (dd, 2H, $J_1 = 9.4$ Hz, $J_2 = 2.5$ Hz), 7.13 (d, 2H, $J = 2.5$ Hz), 7.48–7.58 (m, 3H), 7.78 (dd, 2H, $J_1 = 7.7$ Hz, $J_2 = 1.8$ Hz), 8.28 (d, 2H, $J = 9.4$ Hz) (Figure S11, Supporting Information). ¹³C NMR (75.5 MHz, CDCl_3): δ (ppm) 34.7, 41.47, 41.52, 86.5, 111.0, 112.8, 113.7, 121.1, 121.5, 129.2, 131.4, 132.9, 136.8, 144.0, 155.8, 156.5 (Figure S12, Supporting Information). FTIR (KBr, cm^{-1}): 2359, 2180, 1577, 1386, 1320, 1262, 1219, 1157, 1054, 952, 906, 844, 772, 690. MS (MALDI): 393 (100), 378 (31), 293 (14). UV-vis (CH_3OH), ($c = 1.5 \times 10^{-5}$ mol dm^{-3}): $\lambda_{\text{max}}/\text{nm}$ ($\log \epsilon/\text{M}^{-1} \text{cm}^{-1}$) = 445 (4.04), 472 (4.33), 625 (4.34), 677 (4.79) (Figure S13, Supporting Information). UV-vis (PBS buffer), ($c \sim 1 \times 10^{-5}$ mol dm^{-3}): $\lambda_{\text{max}}/\text{nm}$ (A/a.u.) = 452 (0.66), 475 (0.96), 609 (1.00), 631 (0.94). Fluorescence (CH_3OH , $A(\lambda_{\text{max}} \text{excitation}) \leq 0.1$): λ_{max} (emission) = 705 nm (Figure S13, Supporting Information). HRMS (APCI⁺): calcd for $\text{C}_{28}\text{H}_{29}\text{N}_2$ (M^+) 393.2325, found 393.2315.

Synthesis of 3,7-Bis(*N,N*-dimethylamino)-5,5-dimethylidibenzo[*b,e*]silin-10(5H)-one (2b). 4,4'-Methylene-bis(3-bromo-*N,N*-dimethylaniline) (6). Aqueous formaldehyde (37%, 3.26 mL, 43.5 mmol) was added dropwise to a solution of 3-bromo-*N,N*-dimethylaniline (3, 17.5 g, 87 mmol) in glacial acetic acid (200 mL) over 15 min. The reaction mixture was then stirred at 90 °C for 1 h. Acetic acid was evaporated under reduced pressure, and the residual acid was neutralized with satd aq NaHCO_3 . The obtained residue was extracted with dichloromethane (3 × 50 mL). The combined organic layers were washed with water (2 × 50 mL) and brine (50 mL), dried over MgSO_4 , and filtered. The solvents were removed under reduced pressure, and the resulting red viscous oil was chromatographed (ethyl acetate/*n*-hexane, 1:30, v/v) to give the pure product. Yield: 11.7 g

(65%). White crystalline solid. Mp: 105–107 °C (lit.^{54,55} mp 100–105 °C). ¹H NMR (300 MHz, CDCl₃): δ (ppm) 2.95 (s, 12H), 4.07 (s, 2H), 6.63 (dd, 2H, *J*₁ = 8.6 Hz, *J*₂ = 2.6 Hz), 6.91 (d, 2H, *J* = 8.6 Hz), 7.00 (d, 2H, *J* = 2.6 Hz) (Figure S18, Supporting Information). ¹³C NMR (75.5 MHz, CDCl₃): δ (ppm) 40.0, 40.6, 112.0, 116.4, 125.8, 127.2, 130.9, 150.2 (Figure S19, Supporting Information). FTIR (KBr, cm⁻¹): 2896, 2807, 1608, 1543, 1508, 1442, 1360, 1325, 1232, 1174, 1066, 1021, 958, 906, 829, 805, 796, 736, 669, 669. MS (EI): 414 (48), 412 (100), 410 (51), 395 (4), 368 (4), 333 (10), 331 (12), 317 (6), 315 (6), 288 (8), 286 (8), 272 (2), 252 (63), 251 (71), 237 (24), 235 (21), 214 (25), 212 (26), 208 (53), 192 (11), 165 (31), 152 (9), 132 (28), 125 (27), 104 (18), 89 (12). This compound has also been characterized elsewhere.²⁵

N3,N3,N7,N7,5,5-Hexamethyl-5,10-dihydrodibenzo[b,e]silin-3,7-diamine (7b). This compound was prepared from 4,4'-methylenebis(3-bromo-*N,N*-dimethylaniline) (**6**, 120 mg, 0.29 mmol) according to a known procedure.³² Column chromatography (ethyl acetate/*n*-hexane 1:20 or 1:10, v/v) afforded a relatively pure product (Figures S20 and S21, Supporting Information). Yield: 64.8 mg (72%). Slightly yellowish crystalline solid. Mp: 120–123 °C. ¹H NMR (300 MHz, CDCl₃): δ (ppm) 0.51 (s, 6H, ((CH₃)₂Si<)), 2.98 (s, 12H), 4.01 (s, 2H), 6.79 (dd, 2H, *J*₁ = 8.4 Hz, *J*₂ = 2.8 Hz), 7.05 (d, 2H, *J* = 2.8 Hz), 7.24 (d, 2H, *J* = 8.5 Hz) (Figure S20, Supporting Information). ¹³C NMR (75.5 MHz, CDCl₃): δ (ppm) -2.56 ((CH₃)₂Si<), 39.4, 41.4, 114.4, 117.8, 128.7, 129.6, 136.3, 148.9 (Figure S21, Supporting Information). FTIR (KBr, cm⁻¹): 1583, 1520, 1490, 1299, 1247, 1222, 1175, 814, 771, 669, 650, 579, 527. MS (EI): 310 (100), 309 (80), 295 (36), 293 (18), 266 (77), 254 (19), 253 (16), 251 (10), 210 (8), 208 (8), 154 (20), 147 (16), 139 (14), 126 (13). HRMS (APCI⁺): calcd for C₁₉H₂₇N₂Si (M + H⁺) 311.1938, found 311.1945.

Note: This compound is readily oxidized to the corresponding pyronin **8b** under ambient atmosphere (Scheme 2b). This hampers characterization of a pure compound (especially using ¹³C NMR). Therefore, it was used immediately in the next step without any further purification.

3,7-Bis(*N,N*-dimethylamino)-5,5-dimethyldibenzo[b,e]silin-10(5*H*)-one (2b). Two methods for preparation of this compound were carried out.

Method A. Inspired by a procedure published by Hell and co-workers.²⁴ Powdered potassium permanganate (81 mg, 0.51 mmol) was added portionwise to a solution of *N3,N3,N7,N7,5,5*-hexamethyl-5,10-dihydrodibenzo[b,e]silin-3,7-diamine (**7b**, 57.9 mg, 0.186 mmol) in acetone (30 mL) at 0 °C over 2 h, and the reaction mixture was stirred for 1 h at 0 °C. The reaction progress was monitored by TLC. Another portion of powdered potassium permanganate (81 mg, 0.51 mmol) was then added over 2 h at 0 °C, and the reaction mixture was stirred overnight at 20 °C. Dichloromethane (20 mL) was then added, the mixture was filtered, and the solvents were removed under reduced pressure. Column chromatography (ethyl acetate/*n*-hexane, 1:5, v/v) gave a pure product. Yield: 13.9 mg (23%). Beige crystalline solid.

Method B. Adopted according to procedures by Nagano et al.³² and Hell et al.²⁴ *n*-Butyllithium (2.5 M solution in cyclohexane, 15.1 mL, 37.8 mmol) was added dropwise within 15 min to a solution of 4,4'-methylenebis(3-bromo-*N,N*-dimethylaniline) (**6**, 6.0 g, 14.6 mmol) in dry tetrahydrofuran (100 mL) at -78 °C under dry N₂ atmosphere. The reaction mixture was stirred for 15 min. Dichlorodimethylsilane (2.3 mL, 18.9 mmol) was then added dropwise over a period of 15 min. The reaction mixture was stirred overnight, while the temperature was allowed to rise to 20 °C. The reaction mixture was quenched by dropwise addition of aq HCl (30 mL, 2 M) and subsequently neutralized with satd aq NaHCO₃ (100 mL). The mixture was extracted with CH₂Cl₂ (3 × 50 mL) and dried over MgSO₄, and the solvents were removed under reduced pressure. The obtained crude solid mixture was diluted in acetone (100 mL) and cooled to 0 °C, and potassium permanganate (6.90 g, 43.7 mmol) was added portionwise over the period of 2 h. The reaction mixture was then allowed to warm to 20 °C. When no starting material was observed (usually after an additional 3 h; TLC) manganese(IV) oxide was filtered off through a pad of silica gel, and the solid was thoroughly washed with chloroform

(~ 1.2 L). Mixed filtrates were concentrated under reduced pressure. Column chromatography (*n*-hexane/chloroform/ethyl acetate, 5:1:1, v/v) provided the pure product. Yield: 2.31 g (49%). Slightly greenish solid. Mp: 276.3–278.5 °C. ¹H NMR (300 MHz, CDCl₃): δ (ppm) 0.48 (s, 6H, ((CH₃)₂Si<)), 3.10 (s, 12H), 6.81 (d, 2H, *J* = 2.8 Hz), 6.85 (dd, 2H, *J*₁ = 8.9 Hz, *J*₂ = 2.8 Hz), 8.41 (d, 2H, *J* = 8.9 Hz) (Figure S22, Supporting Information). ¹³C NMR (75.5 MHz, CDCl₃): δ (ppm) -0.8 ((CH₃)₂Si<), 40.2, 113.4, 114.5, 129.9, 131.8, 140.7, 151.7, 185.5 (Figure S23, Supporting Information). FTIR (KBr, cm⁻¹): 1583, 1504, 1364, 1299, 1179, 1150, 1064, 925, 843, 767, 574. MS (EI): 324 (100), 309 (99), 294 (11), 293 (32), 277 (4), 265 (4), 161 (5), 148 (26), 132 (7), 119 (2). HRMS (APCI⁺): calcd for C₁₉H₂₅N₂O₂Si (M + H⁺) 325.1731, found 325.1732. This compound has also been characterized elsewhere.²⁵

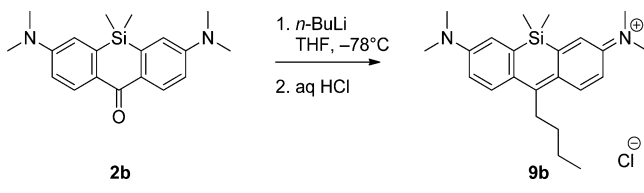
***N*-(7-(Dimethylamino)-5,5-dimethyl-10-(phenylethynyl)dibenzo[b,e]silin-3(5*H*)-ylidene)-*N*-methylmethanaminium Chloride (1b).** *n*-Butyllithium (2.5 M solution in hexanes, 0.62 mL, 1.54 mmol) was added dropwise to a solution of phenylacetylene (0.186 mL, 1.70 mmol) in dry tetrahydrofuran (5 mL) in a Schlenk tube at -78 °C under dry N₂ atmosphere (Scheme 1). The mixture was stirred for 30 min, and a solution of 3,7-bis(*N,N*-dimethylamino)-5,5-dimethyldibenzo[b,e]silin-10(5*H*)-one (**2b**, 100 mg, 0.31 mmol) in dry tetrahydrofuran (10 mL) was added dropwise. The reaction mixture was stirred at -78 °C for 30 min and then stirred overnight while the temperature was allowed to rise to 20 °C. The reaction was quenched by dropwise addition of aq HCl (3 mL, 2 M), and the mixture was extracted with dichloromethane (3 × 20 mL). The combined organic extracts were dried over anhydrous MgSO₄, and the solvents were removed under reduced pressure to give an oily crude product. Column chromatography (methanol/chloroform, 1:20 to 1:8, v/v) gave the pure crystalline product. Yield: 114 mg (83%). Dark green microcrystalline powder. Mp: 221–223 °C. ¹H NMR (300 MHz, CD₃OD): δ (ppm) 0.56 (s, 6H, ((CH₃)₂Si<)), 3.38 (s, 12H), 7.07 (dd, 2H, *J*₁ = 9.5 Hz, *J*₂ = 2.8 Hz), 7.25 (d, 2H, *J* = 2.8 Hz), 7.50–7.59 (m, 3H), 7.76–7.81 (m, 2H), 8.52 (d, 2H, *J* = 9.5 Hz) (Figure S24, Supporting Information). ¹³C NMR (75.5 MHz, CD₃OD): δ (ppm) -1.0 ((CH₃)₂Si<), 41.1, 90.5, 113.2, 116.0, 121.6, 122.7, 129.8, 130.2, 132.4, 133.7, 141.7, 147.2, 149.0, 155.8. (Figure S25, Supporting Information). FTIR (KBr, cm⁻¹): 2937, 2885, 2179, 1577, 1491, 1379, 1317, 1263, 1219, 1180, 1157, 1057, 955, 908, 845, 835, 806, 773, 752, 688, 646, 524. MS (EI): 409 (6), 368 (35), 353 (3), 324 (7), 309 (12), 255 (15), 236 (26), 152 (17), 135 (21), 123 (19), 111 (38), 97 (67), 83 (71), 57 (100). UV-vis (CH₃OH), (*c* = 1.0 × 10⁻⁵ mol dm⁻³): λ_{max}/nm (log ε/M⁻¹ cm⁻¹) 462 (4.08), 490 (4.38), 660 (4.57), 712 (4.91) (Figure S26, Supporting Information). UV-vis (PBS buffer), (*c* ~ 1 × 10⁻⁵ mol dm⁻³): λ_{max}/nm (rel A/a.u.) = 469 (0.72), 492 (1.00), 646 (0.83), 709 (0.56). Fluorescence (CH₃OH, A(λ_{max} excitation)) ≤ 0.1; λ_{max} (emission) = 738 nm (Figure S26, Supporting Information). HRMS (APCI⁺): calcd for C₂₇H₂₉N₂Si (M⁺) 409.2095, found 409.2097.

Caution: Addition of a molar excess of *n*-BuLi provides favorably *N*-(10-butyl-7-(dimethylamino)-5,5-dimethyldibenzo[b,e]silin-3(5*H*)-ylidene)-*N*-methylmethanaminium chloride (**9b**) as a side product (HRMS (APCI⁺): calcd for C₂₃H₃₃N₂Si (M⁺) 365.2408, found 365.2407). We found it inseparable from the title product **1b** by column chromatography on silica (Scheme 4). Therefore, special attention should be taken to avoid unreacted *n*-BuLi in the reaction mixture prior to the ketone addition.

9*H*-Pyronin Analogues. General Procedure. Lithium aluminum hydride (69 mg, 1.85 mmol) was added to a solution of the corresponding xanthenone (**2**, 0.62 mmol) in dry THF (20 mL) in one portion, and the reaction mixture was stirred at 25 °C for 12 h (Scheme 3). Aqueous HCl (3 mL, 2 M) was then added dropwise to the reaction mixture, the solution was saturated with solid NaCl, and the mixture was extracted with dichloromethane (6 × 15 mL). The combined organic extracts were dried over anhydrous MgSO₄ and filtered, and solvents were removed under reduced pressure to give the product.

Note: 9*H*-Pyronin analogues are very soluble in water but only slightly soluble in ethyl acetate and other polar water-immiscible

Scheme 4. Nucleophilic Addition of *n*-Butyllithium on 3,7-Bis(*N,N*-dimethylamino)-5,5-dimethyldibenzo[*b,e*]silin-10(5*H*)-one (2b)



solvents. The compounds decompose on silica. Excess reducing agent is important for obtaining a sufficiently pure product **8**.

N-(7-(Dimethylamino)-9,9-dimethylantracen-2(9*H*)-ylidene)-*N*-methylmethanaminium Chloride (**8a**). The compound was prepared from 3,6-bis(dimethylamino)-10,10-dimethylantracen-9(10*H*)-one (**2a**) according to a general procedure. Yield: 185 mg (87%). Blue powder with a metal gloss. Mp: 147–150 °C. ¹H NMR (500 MHz, CD₃OD): δ (ppm) 1.72 (s, 6H), 3.37 (s, 12H), 7.00 (dd, 2H, *J*₁ = 9.0 Hz, *J*₂ = 2.4 Hz), 7.19 (d, 2H, *J* = 2.4 Hz), 7.72 (d, 2H, *J* = 9.1 Hz), 8.13 (s, 1H) (Figure S31, Supporting Information). ¹³C NMR (125 MHz, CD₃OD): δ (ppm) 34.2, 41.1, 43.3, 112.3, 114.2, 122.2, 140.3, 155.40, 155.44, 158.7. (Figure S32, Supporting Information). FTIR (neat, cm⁻¹) = 2963, 2923, 2863, 2805, 1594, 1560, 1515, 1461, 1425, 1330, 1285, 1157, 1016, 888, 797, 698, 522, 469. MS (MALDI): 293.25 (85), 278.22 (100), 222.17 (9). UV–vis (CH₃OH), (*c* = 2.3 × 10⁻⁵ mol dm⁻³): λ_{max}/nm (log ε/mol dm⁻³ cm⁻¹) = 605 (4.75) (Figure S33, Supporting Information). UV–vis (PBS buffer), (*c* ~ 2.5 × 10⁻⁵ mol dm⁻³): λ_{max}/nm (log ε/M⁻¹ cm⁻¹) = 604 (4.74). Fluorescence (CH₃OH, A(λ_{max} (excitation)) ≤ 0.1): λ_{max} (emission) = 620 nm (Figure S33, Supporting Information). Fluorescence (PBS buffer, A(λ_{max} (excitation)) ≤ 0.1): λ_{max} (emission) = 621 nm. HRMS (APCI⁺): calcd for C₂₀H₂₅N₂ (M⁺) 293.2012, found 293.2008. This compound has also been characterized elsewhere.^{56,57}

N-(7-(Dimethylamino)-5,5-dimethyldibenzo[*b,e*]silin-3(5*H*)-ylidene)-*N*-methylmethanaminium Chloride (**8b**). Prepared from 3,7-bis(*N,N*-dimethylamino)-5,5-dimethyldibenzo[*b,e*]silin-10(5*H*)-one (**2b**) according to a general procedure. Yield: 192 mg (90%). Blue powder with metal gloss. Mp: 193–194 °C. ¹H NMR (500 MHz, CD₃OD): δ (ppm) 0.54 (s, 6H, ((CH₃)₂Si<)), 3.37 (s, 12H), 6.98 (dd, 2H, *J*₁ = 9.2 Hz, *J*₂ = 2.7 Hz), 7.32 (dd, 2H, *J* = 2.7 Hz), 7.72 (d, 2H, *J* = 9.2 Hz), 7.88 (s, 1H) (Figure S34, Supporting Information). ¹³C NMR (125 MHz, CDCl₃): δ (ppm) -1.4 ((CH₃)₂Si<), 41.0, 115.2, 122.2, 128.9, 144.5, 148.9, 156.8, 161.2 (Figure S35, Supporting Information). FTIR (neat, cm⁻¹): 2922, 2875, 2810, 1586, 1541, 1504, 1461, 1422, 1351, 1323, 1298, 1117, 1047, 876, 823, 799, 741, 522, 422. MS (MALDI): 309.22 (100), 310.21 (24). UV–vis (CH₃OH), (*c* = 2.1 × 10⁻⁵ mol dm⁻³): λ_{max}/nm (log ε/M⁻¹ cm⁻¹) = 636 (4.51) (Figure S36, Supporting Information). UV–vis (PBS buffer; *c* ~ 2.1 × 10⁻⁵ mol dm⁻³): λ_{max}/nm (log ε/M⁻¹ cm⁻¹) = 634 (4.86). Fluorescence (CH₃OH, A(λ_{max} (excitation)) ≤ 0.1): λ_{max} (emission) = 648 nm (Figure S36, Supporting Information). Fluorescence (PBS buffer, A(λ_{max} (excitation)) ≤ 0.1): λ_{max} (emission) = 649 nm. HRMS (APCI⁺): calcd for C₁₉H₂₅N₂Si (M⁺) 309.1782, found 309.1779. This compound has also been characterized elsewhere.⁵⁸

■ ASSOCIATED CONTENT

Supporting Information

NMR, UV–vis, and fluorescence data; optimization of the parameters for in vivo applications; images of cells stained by the fluorescent dyes. This material is available free of charge via the Internet at <http://pubs.acs.org>.

■ AUTHOR INFORMATION

Corresponding Author

*E-mail: klan@sci.muni.cz. Tel: +420-54949-4856. Fax: +420-54949-2443.

Notes

The authors declare no competing financial interest.

■ ACKNOWLEDGMENTS

Support for this work was provided by the Czech Science Foundation (13-25775S), the Czech Ministry of Education (LO1214) (P.K.), Masaryk University (MUNI/A/0975/2009; J.M.), and the project “Employment of Best Young Scientists for International Cooperation Empowerment” (CZ.1.07/2.3.00/30.0037) cofinanced by the European Social Fund and the state budget of the Czech Republic. (P.Š.). We express our thanks to Lukáš Maier, Miroslava Bittová, and Lubomir Prokeš for their help with the mass spectrometry and NMR. Ján Krausko and L’ubica Krausková are acknowledged for their help with the fluorescence and UV measurements. The Institute for Biophysics, Academy of Sciences of the Czech Republic, v.v.i., is acknowledged for access to the confocal fluorescence microscope, and Ludmila Šebejová, Tomáš Šolomek, and Jakob Wirz are acknowledged for fruitful discussions.

■ REFERENCES

- (1) Lang, K.; Chin, J. W. *Nat. Chem.* **2013**, *5*, 81.
- (2) Stender, A. S.; Marchuk, K.; Liu, C.; Sander, S.; Meyer, M. W.; Smith, E. A.; Neupane, B.; Wang, G.; Li, J.; Cheng, J.-X.; Huang, B.; Fang, N. *Chem. Rev.* **2013**, *113*, 2469.
- (3) Yang, Y.; Zhao, Q.; Feng, W.; Li, F. *Chem. Rev.* **2012**, *113*, 192.
- (4) Gonçalves, M. S. T. *Chem. Rev.* **2008**, *109*, 190.
- (5) Vendrell, M.; Zhai, D.; Er, J. C.; Chang, Y.-T. *Chem. Rev.* **2012**, *112*, 4391.
- (6) Sun, Y.-Q.; Liu, J.; Lv, X.; Liu, Y.; Zhao, Y.; Guo, W. *Angew. Chem., Int. Ed.* **2012**, *51*, 7634.
- (7) Wysocki, L. M.; Lavis, L. D. *Curr. Opin. Chem. Biol.* **2011**, *15*, 752.
- (8) Beija, M.; Afonso, C. A. M.; Martinho, J. M. G. *Chem. Soc. Rev.* **2009**, *38*, 2410.
- (9) Johnson, L. V.; Walsh, M. L.; Chen, L. B. *Proc. Nat. Acad. Sci. U.S.A.* **1980**, *77*, 990.
- (10) Scaduto, R. C.; Grotyohann, L. W. *Biophys. J.* **1999**, *76*, 469.
- (11) Ward, M. W. In *Live Cell Imaging, Methods and Protocols*; Papkovsky, D. B., Ed.; Springer: New York, 2010; Vol. 591, p 335.
- (12) Loeffler, M.; Kroemer, G. *Exp. Cell Res.* **2000**, *256*, 19.
- (13) Chen, J.; Liu, W.; Zhou, B.; Niu, G.; Zhang, H.; Wu, J.; Wang, Y.; Ju, W.; Wang, P. *J. Org. Chem.* **2013**, *78*, 6121.
- (14) Kolmakov, K.; Belov, V. N.; Bierwagen, J.; Ringemann, C.; Mueller, V.; Eggeling, C.; Hell, S. W. *Chem.—Eur. J.* **2010**, *16*, 158.
- (15) Amat-Guerri, F.; Martin, M. E.; Martinez-Utrilla, R.; Pascual, C. *J. Chem. Res., Synop.* **1988**, 184.
- (16) Stacko, P.; Sebej, P.; Veetil, A. T.; Klan, P. *Org. Lett.* **2012**, *14*, 4918.
- (17) Sebej, P.; Wintner, J.; Mueller, P.; Slanina, T.; Al Anshori, J.; Antony, L. A. P.; Klan, P.; Wirz, J. *J. Org. Chem.* **2013**, *78*, 1833.
- (18) Martínez-Peragón, A.; Miguel, D.; Jurado, R.; Justicia, J.; Álvarez-Pez, J. M.; Cuerva, J. M.; Crovetto, L. *Chem.—Eur. J.* **2014**, *20*, 447.
- (19) Turk, S.; Kovac, A.; Boniface, A.; Bostock, J. M.; Chopra, I.; Blanot, D.; Gobec, S. *Bioorgan. Med. Chem.* **2009**, *17*, 1884.
- (20) Shi, J. M.; Zhang, X. P.; Neckers, D. C. *Tetrahedron Lett.* **1993**, *34*, 6013.
- (21) Klimtchuk, E.; Rodgers, M. A. J.; Neckers, D. C. *J. Phys. Chem.* **1992**, *96*, 9817.
- (22) Antony, L. A. P.; Slanina, T.; Sebej, P.; Solomek, T.; Klan, P. *Org. Lett.* **2013**, *15*, 4552.
- (23) Ustinov, A.; Korshun, V. US Pat. 2012/0316319 A1, 2012.
- (24) Kolmakov, K.; Belov, V. N.; Wurm, C. A.; Harke, B.; Leutenegger, M.; Eggeling, C.; Hell, S. W. *Eur. J. Org. Chem.* **2010**, *2010*, 3593.
- (25) Koide, Y.; Urano, Y.; Hanaoka, K.; Terai, T.; Nagano, T. *ACS Chem. Biol.* **2011**, *6*, 600.

- (26) Valdesaguilera, O.; Neckers, D. C. *J. Phys. Chem.* **1988**, *92*, 4286.
- (27) Toptygin, D.; Packard, B. Z.; Brand, L. *Chem. Phys. Lett.* **1997**, *277*, 430.
- (28) Antonov, L.; Gergov, G.; Petrov, V.; Kubista, M.; Nygren, J. *Talanta* **1999**, *49*, 99.
- (29) Arbeloa, F. L.; Gonzalez, I. L.; Ojeda, P. R.; Arbeloa, I. L. *J. Chem. Soc., Faraday Trans. 2* **1982**, *78*, 989.
- (30) Sauer, M.; Hofkens, J.; Enderlein, J. *Handbook of Fluorescence Spectroscopy and Imaging: From Ensemble to Single Molecules*; Wiley-VCH: Weinheim, 2011.
- (31) Haugland, R. P. In *Current Protocols in Cell Biology*; Wiley: New York, 2001; p 16.5.1.
- (32) Egawa, T.; Koide, Y.; Hanaoka, K.; Komatsu, T.; Terai, T.; Nagano, T. *Chem. Commun.* **2011**, *47*, 4162.
- (33) Urano, Y.; Kamiya, M.; Kanda, K.; Ueno, T.; Hirose, K.; Nagano, T. *J. Am. Chem. Soc.* **2005**, *127*, 4888.
- (34) Weissleder, R.; Ntziachristos, V. *Nat. Med.* **2003**, *9*, 123.
- (35) Berlier, J. E.; Rothe, A.; Buller, G.; Bradford, J.; Gray, D. R.; Filanoski, B. J.; Telford, W. G.; Yue, S.; Liu, J. X.; Cheung, C. Y.; Chang, W.; Hirsch, J. D.; Beechem, J. M.; Haugland, R. P. *J. Histochem. Cytochem.* **2003**, *51*, 1699.
- (36) Escobedo, J. O.; Rusin, O.; Lim, S.; Strongin, R. M. *Curr. Opin. Chem. Biol.* **2010**, *14*, 64.
- (37) Neugebauer, U.; Pellegrin, Y.; Devocelle, M.; Forster, R. J.; Signac, W.; Morand, N.; Keyes, T. E. *Chem. Commun.* **2008**, 5307.
- (38) Martin, A.; Long, C.; Forster, R. J.; Keyes, T. E. *Chem. Commun.* **2012**, *48*, 5617.
- (39) Araneda, J. F.; Piers, W. E.; Heyne, B.; Parvez, M.; McDonald, R. *Angew. Chem., Int. Ed.* **2011**, *50*, 12214.
- (40) Pham, W.; Cassell, L.; Gillman, A.; Koktysh, D.; Gore, J. C. *Chem. Commun.* **2008**, 1895.
- (41) Baathulaa, K.; Xu, Y.; Qian, X. *J. Photochem. Photobiol. A* **2010**, *216*, 24.
- (42) Burghart, A.; Thoresen, L. H.; Chen, J.; Burgess, K.; Bergstrom, F.; Johansson, L. B. A. *Chem. Commun.* **2000**, 2203.
- (43) Loudet, A.; Ueno, Y.; Wu, L.; Jose, J.; Barhoumi, R.; Burghardt, R.; Burgess, K. *Bioorg. Med. Chem. Lett.* **2011**, *21*, 1849.
- (44) Shcherbakova, D. M.; Hink, M. A.; Joosen, L.; Gadella, T. W. J.; Verkhusha, V. V. *J. Am. Chem. Soc.* **2012**, *134*, 7913.
- (45) Gottlieb, H. E.; Kotlyar, V.; Nudelman, A. *J. Org. Chem.* **1997**, *62*, 7512.
- (46) Samanta, D.; Sawoo, S.; Patra, S.; Ray, M.; Salmain, M.; Sarkar, A. *J. Organomet. Chem.* **2005**, *690*, 5581.
- (47) Okamoto, Y.; Brown, H. C. *J. Am. Chem. Soc.* **1958**, *80*, 4976.
- (48) Oki, M.; Iwamura, H. *Bull. Chem. Soc. Jpn.* **1962**, *35*, 1552.
- (49) Ujttewaal, A. P.; Jonkers, F. L.; Van der Gen, A. *J. Org. Chem.* **1979**, *44*, 3157.
- (50) Reynolds, W. F.; Gomes, A.; Maron, A.; MacIntyre, D. W.; Maunder, R. G.; Tanin, A.; Wong, H. E.; Hamer, G. K.; Peat, I. R. *Can. J. Chem.* **1983**, *61*, 2367.
- (51) Naimi-Jamal, M. R.; Mokhtari, J.; Dekamin, M. G.; Kaupp, G. *Eur. J. Org. Chem.* **2009**, *2009*, 3567.
- (52) Shaikh, N. S.; Junge, K.; Beller, M. *Org. Lett.* **2007**, *9*, 5429.
- (53) Lundgren, R. J.; Sapping-Kumankumah, A.; Stradiotto, M. *Chem.—Eur. J.* **2010**, *16*, 1983.
- (54) Bychkov, N. N.; Negrebetskii, V. V.; Kostitsyn, A. B.; Stepanov, B. I. *Russ. J. Gen. Chem.* **1984**, *54*, 1995.
- (55) Gorvin, J. H. *J. Chem. Soc.* **1953**, 1237.
- (56) Arden-Jacob, J.; Frantzeskos, J.; Kemnitzer, N. U.; Zilles, A.; Drexhage, K. H. *Spectrochim. Acta A-M* **2001**, *57*, 2271.
- (57) Aaron, C.; Barker, C. C. *J. Chem. Soc.* **1963**, 2655.
- (58) Fu, M.; Xiao, Y.; Qian, X.; Zhao, D.; Xu, Y. *Chem. Commun.* **2008**, 1780.